Pixel-by-Pixel Spatiotemporal Progression of Focal Ischemia Derived using Quantitative Perfusion and Diffusion Imaging

Q. Shen[1], X. Meng[2], M. Fisher[2,3], C. H. Sotak[3,4], T. Q. Duong[1]

[1]Center for Comparative NeuroImaging, Department of Psychiatry, University of Massachusetts Medical School, Worcester, MA, United States, [2]Department of Neurology, University of Massachusetts Medical School, Worcester, MA, United States, [3]Department of Radiology, University of Massachusetts Medical School, Worcester, MA, United States, [4]Departments of Biomedical Engineering and Chemistry & Biochemistry, Worcester Polytechnic Institute, Worcester, MA, United States

Introduction Although the "perfusion-diffusion mismatch" had been widely observed in acute human stroke [1], similar observations in animal stroke models are limited and the temporal evolution of the perfusion-diffusion mismatch in animal models has yet to be systematically investigated. Animal models where focal ischemia can be reproducibly studied under controlled conditions would be important for identifying and predicting the severity of ischemic injury and for evaluating the efficacy of therapeutic intervention [2]. In this study, we utilized *quantitative* perfusion and diffusion imaging to investigate the *temporal* and *spatial evolution* of focal ischemia following permanent intraluminal middle cerebral artery occlusion (MCAO) in rats during the acute phase. We focused on quantitative perfusion and diffusion imaging of the acute phase because proton density (given by M_0), T_1 and T_2 relaxation times are generally unaffected early after stroke onset and only begin to change with the advent of vasogenic edema (i.e., typically > 4 hours) [3]. The goal of this study was to evaluate *pixel-by-pixel* the temporal and spatial evolution of permanent focal ischemia during the acute phase using combined diffusion and perfusion analysis. These results were correlated with histology at 24 hrs post-ischemia.

Method Eleven male SD rats (300-350g) were initially anesthetized with chloral hydrate (400mg/kg, ip). Permanent focal ischemia was induced using the intraluminal middle cerebral artery occlusion (MCAO) method. The right femoral artery was catheterized for blood-gas sampling and continuous monitoring of blood pressure and heart rate. Anesthesia was switched to 1% isoflurane during MRI. The rectal temperature was kept at 37.0±0.5°C. MRI data were acquired every 30 mins for 3 hours, and followed by TTC staining at ~24 hrs post-occlusion. MRI was performed on a 4.7T/40cm magnet. ADC(trace) was measured using spin-echo EPI with matrix = 64x64, FOV = 2.5cm x1.9cm, seven 1.5-mm slices, TE = 43ms, TR = 2s, 16 averages, b = 10, 1504 s/mm^2 along each of the 3 principle axes. CBF was measured using the continuous arterial spin-labeling technique with single-shot, gradient-echo EPI, with parameters similar to the ADC measurement except TE = 15ms. ADC(trace) and CBF images were calculated at each time point. Lesion volumes (LV's) were derived using the CBF (57±11 % reduction, 0.30±0.09 ml/g/min, n = 5) and the ADC (30±2% reduction, 0.53±0.03 x10^{-3}mm^2/s) viability thresholds established previously [4]. Pixel-by-pixel CBF-ADC scatter plots were analyzed at each time point.

Results & Discussions Fig. 1a shows the CBF-ADC scatterplots from one animal. The ADC-CBF distributions of the left hemisphere (LH) were markedly different from those of the right hemisphere (RH) at 30 and 180 mins. In contrast to the single cluster in the normal LH, multiple clusters were observed in the ischemic RH and four zones were operationally defined based on the TTC-derived ADC and CBF thresholds: *i)* the "normal" cluster with normal CBF and ADC; *ii)* the "core" cluster with marked reduced CBF and ADC; *iii)* the "mismatch" cluster with reduced CBF but slightly reduced ADC, and *iv)* zone 4. Essentially no pixels fell in "zone 4".

Pixels from the three zones were color-coded and mapped onto the image space (**Fig. 1b**). At 30 mins post-ischemia, the mismatch pixels (yellow) were substantial. As time evolved, the mismatch area decreased and, at 180 mins, the majority (~80%) of the mismatch pixels had migrated into the core (orange); the remaining ~20% presumably arose from viable tissues with normal ADC but mild and sustained CBF reduction. The normal zone, on the other hand, was relatively time invariant. The "ischemic core" pixels (orange) grew as ischemia progressed and essentially all came from the mismatch zone. The detailed history of the core pixels at various time points is shown in **Fig. 1c**. In the ADC-CBF space, pixels that eventually became infarcted predominantly (90%) came from the mismatch zone, whereas only 10% of the pixels came from the normal zone. In the image spaces, ischemia developed predominantly medial and peripheral to the initial ischemic core. **Fig. 2** shows the volume evolutions of the three clusters.

Volume evolutions of the mismatch pixels at 30 mins as they evolved into different zones are shown in **Fig. 3.** By definition, the mismatch pixels at 30 mins was maximum. As ischemia evolved, the mismatch volume decreased and, at 180 mins post-ischemia, it reached 20% of the volume at the 30-min time point. The remaining mismatch pixels at 180 mins were likely to be viable tissues with normal ADC but sustained (mild) CBF reduction and/or inter-subject variation. ADC-(230±50 mm^3) and CBF-defined (230±40 mm^3) LV at 3hrs was not statistically significant from the TTC infarct volumes at 24hrs (220±40 mm^3) (P>0.05).

Projection profiles of the ADC and CBF distributions were analyzed. In contrast to the LH, the RH ADC distribution was bimodal with a distinct separation (a minimum); such minima did not substantially change with time (**Fig. 4a**). The ADC biomodal minimum ($ADC_{bimodal}$) was -24% reduction (0.57±0.02 x10^{-3} mm^2/s) and the corresponding CBF value ($CBF_{bimodal}$) -56% reduction (0.35±0.04 ml/g/min), were surpringly similar to the TTC-derived viability thresholds [4]. The mean left-mode RH ADC (0.47±0.07 x10^{-3} mm^2/s) was markedly lower than the LH ADC and shifted to a lower ADC as ischemia progressed, whereas the mean right-mode RH ADC (0.71±0.07 x10^{-3} mm^2/s) was similar to the LH ADC and did not shift with time. The left-mode ADC volume increased and the right-mode ADC volume decreased as ischemia progressed. In regards to CBF distributions, the RH CBF was markedly lower than the LH CBF as expected. The RH CBF profiles were uni-modal and, thus, different clusters could not be readily resolved based on CBF differences alone (**Fig. 4b**).

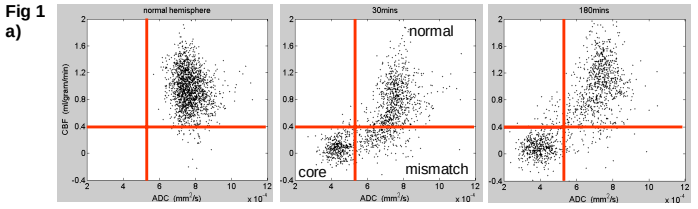

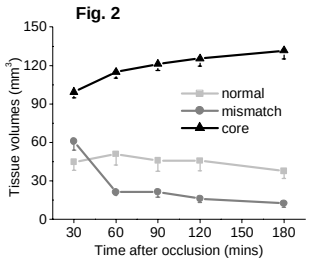

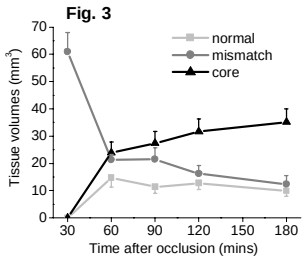

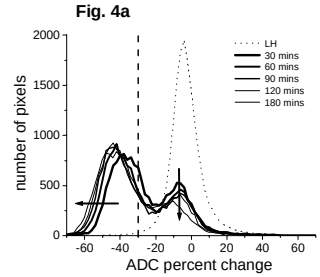

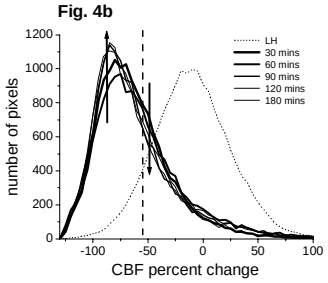

Conclusions This study established a quantitative imaging and a pixel-by-pixel analysis protocol to evaluate the spatio-temporal evolution in the CBF-ADC and image spaces of ischemic brain injury during the acute phase. This analysis approach is expected to provide a powerful tool to evaluate drug efficacy, and potentially offer a means to make statistical prediction of ischemic tissue fates.

References [1] Baird AE, Ann Neurol 41: 581; [2] Neumann HT, Stroke 30: 1591; [3] Fisher M, Neurology 52: 1750; [4] Meng et al., ISMRM 2003, 1:303.